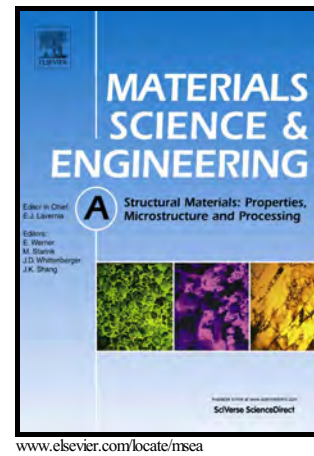


Author's Accepted Manuscript

Reinforcing effects of carbon nanotube on carbon/carbon composites before and after heat treatment

Liyuan Han, Kezhi Li, Jiajia Sun, Qiang Song, Yawen Wang



PII: S0921-5093(18)31081-5
DOI: <https://doi.org/10.1016/j.msea.2018.08.025>
Reference: MSA36796

To appear in: *Materials Science & Engineering A*

Received date: 8 June 2018
Revised date: 7 August 2018
Accepted date: 9 August 2018

Cite this article as: Liyuan Han, Kezhi Li, Jiajia Sun, Qiang Song and Yawen Wang, Reinforcing effects of carbon nanotube on carbon/carbon composites before and after heat treatment, *Materials Science & Engineering A*, <https://doi.org/10.1016/j.msea.2018.08.025>

This is a PDF file of an unedited manuscript that has been accepted for publication. As a service to our customers we are providing this early version of the manuscript. The manuscript will undergo copyediting, typesetting, and review of the resulting galley proof before it is published in its final citable form. Please note that during the production process errors may be discovered which could affect the content, and all legal disclaimers that apply to the journal pertain.

Reinforcing effects of carbon nanotube on carbon/carbon composites before and after heat treatment

Liyuan Han^{1*}, Kezhi Li¹, Jiajia Sun¹, Qiang song^{1,2}, Yawen wang¹

¹ *State Key Laboratory of Solidification Processing, Carbon/Carbon Composites Research Center, Northwestern Polytechnical University, Xi'an 710072, China*

² *Center for Nano Energy Materials, Northwestern Polytechnical University, Xi'an 710072, China*

Abstract: Different contents of carbon nanotubes (CNTs) were in situ grown on the surface of carbon fiber bundles by injection chemical vapor deposition. The fibers were then stacked into unidirectional preforms and densified by pyrocarbon (PyC) via chemical vapor infiltration. The effects of CNT on the strength and toughness of carbon/carbon composites (C/Cs) before and after heat treatment at 2100°C were investigated. Results show that both the tensile strength and work of fracture achieves the optimum performance when the CNT content is 1.5 wt%. After heat treatment, the tensile strength increases by 25.68% for CNT reinforced C/Cs (CNTs-C/Cs), while only 4.36% for pure C/Cs. The refinement effect of CNT promotes the resistance of PyC matrix against destruction and makes it maintain the structural integrity and continuity even after heat treatment. Before heat treatment, the presence of CNT results in a decreased in-plane lattice size (L_a) compared with pure C/Cs. while interestingly, after heat treatment, L_a becomes larger due to the stress graphitization of CNT. The stress graphitization induced by CNT gives the carbon matrix a stronger ability to resist crack propagation, thereby

*Corresponding author. Tel.: +86-29-88495764; E-mail address: 296357961@qq.com (Liyuan Han).

enhancing the strength of the C/Cs. In addition, the existence of CNT changes the fracture mode of the C/Cs and increases the way of energy consumption during the tensile test. Thus, both fibers and the interface of the composites are fully utilized.

Keywords: carbon nanotubes; induced graphitization; carbon/carbon composites; tensile strength; heat treatment

1. Introduction

Carbon/carbon composites (C/Cs) are widely used as ultrahigh temperature structural materials in aeronautics and astronautics[1, 2]. Due to the inherent features of carbon matrix including large brittleness and low strength, the mechanical properties of C/Cs are far from satisfactory for the application of advanced aculeated or thin components in the next generation of aerospace systems[3, 4]. Carbon nanotubes (CNTs) possess exceptionally high stiffness and strength[5-8], which are regarded as the efficient nanoscale reinforcements to strengthen and toughen C/Cs beyond microscale carbon fibers.

At present, the most frequently used method for introducing CNT into C/Cs is in-situ growth method using catalysis chemical vapor deposition (CCVD)[9], which can improve uniformity of CNT on carbon fibers and control CNT yielding, length and orientation. But carbon fibers are damaged during CNT growth due to acid treatment and high-temperature etches of metal particles, which leads to the decrease of fiber dominated mechanical properties[10]. Therefore, most researches have been only focused on the effects of CNTs on matrix dominated mechanical properties of C/Cs[11, 12], and almost no work is available to fiber dominated mechanical properties, especially for the tensile performance which is really

important to the employ of C/Cs. Therefore, it is urgent to study the effect of CNT on the tensile property of C/Cs and the influencing mechanism.

Injection chemical vapor deposition (ICVD) has been proved to be an efficient process for synthesizing CNT with controllable length and orientation[13]. Compared with CCVD process, which needs catalyst to be carried on the fiber surface firstly, ICVD process involves the simultaneous pyrolysis of the catalyst precursor and the carbon source. Thus, avoiding acid erosion and high-temperature treatment, ICVD process can reduce mechanical degradation of carbon fibers as far as possible and improve the fiber dominated mechanical properties of composites.

In principle, the great designability of CNT reinforced C/Cs would provide a large potential to achieve a simultaneous reinforcement to the whole matrix and the fiber and matrix (F/M) interface[14-16], and this can optimize the global performance of materials and promote their application in enlarged fields. To scientifically investigate the tensile property of CNT reinforced C/Cs (CNTs-C/Cs), a model of unidirectional C/Cs has been selected. Besides, graphitization as a post-treatment after the infiltration process has great influence on the structure change of pyrocarbon (PyC) and F/M interface binding force[17, 18]. A comparison of structure and properties of composites before and after heat treatment is beneficial to explain the strengthening and toughening mechanisms of CNT during the tensile tests. In this work, different contents of CNT are doped in composites to find the optimal containing of CNT reinforcement and maximize the tensile strength of C/Cs, and then detailed fracture mechanisms are illuminated. A graphitization of 2100°C is an assistant strategy for analysing

the role of CNT in the process of structure change on micro- and nano-scale, which is a supplementary explanation to the tensile behaviors of CNTs-C/Cs.

2. Experimental

2.1 Composites preparation

Unidirectional 3K carbon fibers (PAN-based T300, Jilin Carbon Corporation, China) with diameters of 6-7 μm were used as the preforms. The carbon fiber bundles were deposited a thin PyC layer by chemical vapor infiltration (CVI) process for 40 min. A flowing mixture of CH_4 (40 L/h) and N_2 (160 L/h) was used during the CVI process with the temperature of 1080°C under the ambient pressure. CNTs were grown on the PyC-coated carbon fibers by injected chemical vapor deposition (ICVD) process at 800°C. A feeding mixture solution consisting of 1.2 wt% ferrocene, 78 wt% ethanol and 20.8 wt% EDA was injected continuously into reaction tube at a rate of 9 mL/h, and argon (Ar) were used as the inert gas with a flow rate of 6 L/h.

According to mass change of PyC-coated carbon fibers before and after CNTs growth, the weight fractions of CNT in C/Cs were calculated. The samples prepared were named as CNTs-C/Cs-x in which -x indicates the content of CNT (wt%) in composites. Finally, the carbon fiber bundles with and without CNT were gathered and densified by CVI for 150 h. Then the specimens were all machined into the size of 75×8×4 mm³ and a part of them were graphitized at 2100°C for 1.5 hours under the protection of Ar for further investigation. There are four kinds of composites namely C/Cs, CNTs-C/Cs, HT-C/Cs and HT-CNTs-C/Cs in which HT- means heat treatment at 2100°C.

2.2 Tensile tests

The tensile tests of composites with and without CNT were measured by universal testing machine (CMT5304-30kN) with a loading speed of 0.5 mm/min, and the gauge length was 20 mm. There were not less than ten valid data for each series.

2.3 Analytical method

Transmission electron microscopy (TEM, Tecnai F30G²) was used to examine the microstructure of CNT. Scanning electron microscopy (SEM, JSM-6700) was utilized to characterize the morphology of CNT on carbon fibers and fracture surface of samples. The samples were also observed by leica DMLP optical microscope in order to identify the polarization microstructure (PLM) of PyC. Raman spectroscopy (Renishaw Invia RM200) was used to characterize the microstructure of PyC using an Ar ion laser with the wavelength of 514.5 nm at room temperature.

3. Results and discussion

3.1 Morphology and microstructure of fibers and composites with CNT

Fig. 1 presents SEM images of carbon fibers with different CNT contents. It is clearly that CNTs are uniformly grown on the fiber surface with a high purity and barely encapsulated carbon particles and become denser as the content increases (Fig. 1(a)-(c)). High magnification SEM image shows that CNT has a curve body with extending morphologies, forming a three-dimensional (3D) network structure around the fibers (Fig. 1(d)), which is beneficial to the reinforcing role of CNT. TEM observation shows that CNTs have bamboo-like structures with outer diameters of 20-70nm and tube-wall thickness of 6-20 nm (Fig. 1(e)). High-resolution TEM image reveals that graphite layers are parallel to the tube axis (Fig. 1(f)),

indicating a high crystallinity.

CNT doped carbon fiber preforms have been densified by CVI for preparing CNT reinforced C/Cs and the microstructures of the composites are investigated by PLM and Raman. Fig. 2(a) and (b) show the PLM images of pure C/Cs and CNTs-C/Cs. In CNTs-C/Cs, the matrix is divided into two layers. Due to the high specific surface area of CNT, there forms refined small particles PyC matrix in the area where there are abundant CNTs next to the fibers[19]. The PyC matrix has a fairly low optical activity which can be classified as isotropic (ISO) PyC. In the area far from the fibers, medium texture PyC exists, showing smaller size particles than in pure C/Cs. Due to the mismatch of coefficient of thermal expansion between carbon fibers and matrix during the process of cooling, there are plenty of annular cracks in pure C/Cs, and in HT-C/Cs both number and size of cracks increase (Fig. 2(c)). However in CNTs-C/Cs, cracks are restrained because of the numerous CNTs and refined PyC particles. CNT in composites not only changes morphologies of PyC into smaller size but helps to restrain the formation of cracks even after heat treatment.

Raman spectroscopy is used to evaluate the effect of CNT on the structure of PyC on the microscale before and after heat treatment. Fig. 3(a) shows the typical Raman spectra of four kinds of C/Cs. All the first order Raman spectra can be mainly deconvoluted into five sub-peaks at 1190 cm^{-1} , 1350 cm^{-1} , 1510 cm^{-1} , 1591 cm^{-1} and 1621 cm^{-1} , which are assigned to TPA, D, A, G and D', as illustrated in Fig. 3(b). In order to investigate the influence of CNT before and after 2100°C heat treatment, parameters obtained from Raman spectra are shown in Table 1. Spectral features for C/Cs doped by different contents of CNT show that there is no

obvious difference between them so that CNTs-C/Cs with 1.5 wt% CNT is used for analysis.

Two prominent bands (D and G band) in Fig. 3 indicate the existence of sp^2 -phase. The G band around 1591 cm^{-1} which corresponds to a perfect graphite crystal structure is assigned to zone center phonons of E_{2g} symmetry[20]. The D band around 1350 cm^{-1} is assigned to K-point phonons of A_{1g} symmetry[21], and it is a result of the breathing modes of sp^2 rings which requires defects for its activation by double resonance[21, 22]. So the D band is related to the presence of structure defects such as distortions, heteroatoms and edges which destroy the regularity of structure. The full width at half maximum intensity of the G band (FWHM-G) is used to reflect the surface crystallinity of carbon material. Yoshida et al. investigated the relationship between FWHM-G and the interlayer spacing d_{002} which shows that the narrower the G band is, the lower the d_{002} gets[23]. The D/G intensity ratio (I_D^*/I_G^*) is a specific parameter to characterize the in-plane lattice sizes (La) and is inversely proportional to it. Knight and White have summarized an empirical expression for using $\lambda=514.5\text{ nm}$ laser line based on Tuinstra and Koenig's original data: $La=4.4/(I_D^*/I_G^*)$. Table 1 lists I_D^*/I_G^* , La and FWHM-G for four kinds of samples. As can be seen, for as-deposited samples there is an increase of I_D^*/I_G^* ratio after introducing CNT into C/Cs which means a smaller La . However, a simultaneous decrease of FWHM-G is evidence that the level of defect decreases and d_{002} is smaller in CNTs-C/Cs. During the CVI process CNT with π - π conjugated electronic structure acts as nuclei of small hydrocarbon molecules, and the big π orbits formed by sp^2 hybridization attract similar-structured small polyaromatic molecules by Van Der Waals forces and induce them arrange parallel to each other then deposit in the direction vertical to CNTs surfaces.

That's the reason why the out-of-plane stacking of PyC in CNTs-C/Cs is more orderly[20]. From the change of I_D^*/I_G^* and FWHM-G, it's interesting to see the presence of CNT makes a shrink of in-plane crystallite size but a decrease of interlayer spacing. After heat treatment at 2100°C, the FWHM-G of both materials decreases to 34 and 28 cm^{-1} indicating a dramatically eliminating of defects especially an out-of-plane disorder. The sharper decrease of I_D^*/I_G^* ratio in CNTs-C/Cs offers a bigger in-plane crystallite size. And this is because in CNTs-C/Cs during the annealing process, different extent of shrinkage results an accumulation of stress which is called stress graphitization, and it helps accelerate the lateral extension of layers and contributes to the crystallite growth[24-26]. Annealing can help CNT refine the structure of PyC both in plane and out of plane which means an improvement of graphitization degree of composites.

In addition to the D and G band, the 1190 cm^{-1} band is assigned to a local vibration mode of the transpolyacetylene-like (TPA) structures which exists at the zigzag edges of defective graphene. The TPA band intensity is supposed to be proportional to the amounts of zigzag chains in graphene layers[27]. The A band in 1510 cm^{-1} is broad dispersion and often assigned to the amorphous carbon which exists in the planes of the aromatic rings with the sp^3 links in the interstitial disordered carbons. Besides, the odd-membered carbon rings or complex assembled clusters can also lead to the presence of A band[27-29]. The D' band in 1621 cm^{-1} , arises from an intra-valley process, is an indication of the presence of edges. According to Cancado's study[30], the D' band has the same intensity in both armchair and zigzag structure so the D' band is independent of the edges structure while the D band shows a dependence with

strong intensity for armchair and weak intensity for zigzag edges. Integrated intensity of TPA band in 1170 cm^{-1} , A band in 1520 cm^{-1} and D' band in 1621 cm^{-1} are normalized for some practical purpose as shown in Table 1. In CNTs-C/Cs, three above-mentioned parameters are lower than those of C/Cs, referring to lower contents of TPA-like chains, sp^3 phase and edges (zigzag and/or armchair structure) after introducing CNT, respectively. Especially, the sharp decrease of I_A/I_G is a signal that sp^3 phase changes into sp^2 and that's a dramatically refinement of PyC structure due to the decrease of amorphous phase. After heat treatment, all of three parameters get lower. Notice that both HT-C/Cs and HT-CNTs-C/Cs have a few content of each kind of defects, it is evident that the rest of them are tough to remove and must be in higher temperature. Considering that both the value of I_{TPA}/I_G and $I_{D'}/I_G$ are approximate in HT-C/Cs and HT-CNTs-C/Cs, it is obvious that after heat treatment the presence of CNT can't influence the edges content. However, in HT-CNTs-C/Cs the value of I_A/I_G is a little bit lower than that of pure HT-C/Cs, and the main explanation is that heat treatment enhances the ability of CNT to eliminate the sp^3 phase, which is beneficial to improve the degree of graphitization and the load-bearing capability of carbon matrix.

3.2 Tensile behaviors of as-deposited composites

The influences of CNT contents on the composites properties are investigated. Fig. 4(a) presents typical stress-strain curves of C/Cs doped with different CNT contents. In CNTs-C/Cs, it is observed in the beginning of tensile test the slope of the curve is much higher than pure C/Cs. It is a signal that CNT strengthen and attach high elastic stiffness to C/Cs[31] which is assessed by Young's modulus. Another observation is that the fracture mode changes from

typical brittle fracture to pseudo-plastic fracture due to the presence of CNT, thus indicating the toughness improvement of composites. Fig. 4(b) illustrates the relationship between tensile strength of CNTs-C/Cs and CNT contents. The tensile strength of the composites increases with the increasing CNT contents from 0 to 1.5 wt%, and then decreases as the content further increases to 2.4 wt%. Compared with pure C/Cs in Table 2, CNTs-C/Cs tensile strength increases by 14.2% and 30.5%, for 0.9 wt% and 1.5 wt% of CNT contents, respectively. When the CNTs content reaches 2.4 wt%, there is a distinct decline of strength and it decreases by 18.3% for 2.4 wt% of CNT content. This may be related to the apparent densities of composites listed in Table 2, it is clearly that CNTs-C/Cs-2.4 has lower density compared with pure C/Cs and other CNTs-C/Cs. A possible reason is that overmuch CNTs hinder the infiltration of PyC into the 3D networks, leading to the formation of a thick PyC matrix shell surrounding the fibers that further causes a decreased strength. It clearly reveals that it is crucial to control the content of CNT on carbon fibers and moderate amount of CNT can optimize the performance of CNTs-C/Cs.

In this work, the toughness of the composites is evaluated by means of the work of fracture, obtained by integration of tensile stress–strain curves. Young's modulus and work of fracture acquired from experiment for C/Cs with different contents of CNT are showed in Table 2 and Fig.5. As can be seen, Young's modulus as well as work of fracture presents an upgrade firstly then descending latter tendency with the contents of CNT increasing and reach their maximum value of 3.84 GPa and 3423.4 KJ/m³ both in CNTs-C/Cs-1.5. The modulus increases by 13.4%, 23.6% and 7.6% for CNT contents of 0.9 wt%, 1.5 wt% and 2.4 wt% compared with

the CNT-free sample, respectively. The work of fracture increases by 71.5% and 190.3% for CNTs-C/Cs-0.9 and CNTs-C/Cs-1.5 compared with the pristine C/Cs. And the value sharply drops below the initial value when the content of CNTs reaches 2.4 wt%. In fact, the increase of work of fracture is influenced by both tensile strength and the strain during the test of samples. As can be seen in Fig.4(a), after the introducing of CNT with 0.9 wt% and 1.5 wt% there is increase of tensile strength but more distinct increase of strain. As a result, the change of strain promotes the increase of work of fracture in a more significant way. Therefore, the tensile strength and work of fracture increase in varying degree. CNT is of great importance to the improvement of the above-mentioned parameters. In the tensile tests, CNT contributes to higher modulus by hindering the propagation of cracks and then suffering the load transferred from matrix, and pull-out of CNT from matrix during the process increases the dissipation of energy. Thus, there is an increase of work of fracture which suggests a preferable toughness. It is clearly that proper content of CNT has promoting effect on the stiffness and toughness of composites, but overmuch CNTs can make negative contribution because of the relative brittle fracture formed in the high-content CNT composites.

3.3 Fracture morphology of as-deposited composites

The role of CNT in improving tensile strength of C/Cs is mainly discussed in this part. SEM images of typical fracture of tested samples are displayed in Fig.6. In pure C/Cs in Fig. 6(a) the fracture surfaces are smooth with little fiber pull-out. This reveals a brittle fracture which shows a considerable interfacial cohesion due to the strong bonding between the fibers and matrix. The load is firstly applied to the large-sized PyC in pure C/Cs with no inhibition to

destructive cracks. The annular cracks in matrix connect to each other and accelerate the propagation of cracks. Then the load is transferred to fibers through the strong bonding interface, and the fibers are snapped in a flash which leads to a breakage of the composites. Fig. 6(b) and (c) show that in CNTs-C/Cs-0.9 and CNTs-C/Cs-1.5 there are a lot of fibers pulled out from matrix which causes a pseudo-plastic fracture. The main explanation for the change is the presence of CNT 3D networks results in a layer of porous matrix around fibers. The pores in nanoscale formed during the CVI process make it easy to connect micro-cracks with each other and deflect to the axial direction of fibers. For the extensive fiber pull-out, it increases the consumption of fracture energy when the fibers debond from matrix, and this reduces the energy used for propagation of cracks and breakage of composites. CNT moderates the interface and creates new channels for energy consumption, and these can be toughening mechanisms of CNT to improve the mechanical performance. However, excess CNT would reduce the mechanical properties of composites, resulting in a relatively brittle fracture in the composites (Fig. 6(d)). It hence can be deduced that in order to improve mechanical performance of composites the content of CNTs cannot increase too much.

Fig. 7 compares magnification SEM micrographs of CNTs-C/Cs and their pure counterparts. Fig. 7(a) shows concentric and platelike PyC matrix around the fibers which is almost neat as a proof of brittle fracture. However, the fracture surfaces of CNTs-C/Cs are rougher and more uneven which results in an increasing surface area of fracture, it means that CNT makes fracture process suffer a larger area in total and more energy is dissipated. This may be a complementary mechanism to toughness[31]. There is a lot of CNTs pull-out as

shown in Fig. 7(b) in the fracture surface of CNTs-C/Cs. CNTs are snapped during the tensile tests, there are some fractured CNTs (white arrows) and some pores (yellow arrows) left by pulled CNTs. It is indeed speculated that additional dissipation of energy on nanoscale has introduced due to the presence of uniformly dispersed CNT. Three mechanisms are raised to describe the role of CNT during the tensile. Firstly, CNT bears a part of load directly together with PyC matrix, and this is responsible for a longer elastic stage of stress-strain curves in Fig. 4. Secondly, when stress transfers from matrix to fibers the CNT 3D network which is infiltrated by PyC as a buffer layer delays the fibers suffering the load directly[32]. In the fracture process CNT changes the direction of crack propagation and make a rougher fracture surface. And thirdly, when the composites are broke lots of CNTs are pulled out from the matrix accompanied by breakages of CNT, leading a significant dissipation of energy. The behaviors of CNT mentioned above partake a portion of load and provide additional source of energy dissipation indeed. As can be seen in Fig. 7(c) and (d) in CNTs-C/Cs-2.4, there are plenty of pores on microscale in the PyC matrix next to fibers. One of the possible reasons for these pores is that superabundant CNTs hinder the infiltration of PyC, and it is easy to form thick matrix with high porosity. During the tensile test these pores on the one hand may lead a stress concentration and accelerate the propagation of cracks from the origin, and on the other hand they make a porous matrix with low bearing capacity. These two reasons make that the tensile strength of CNTs-C/Cs-2.4 is the lowest among the four CNT enhanced composites.

In pure C/Cs, the load is on matrix first and then transfers to the fibers immediately, as a result the fracture happens in an instant corresponding to a brittle fracture. However in

CNTs-C/Cs, CNT with moderate amounts change the style of loading transfer and tensile fracture. Among the reasons for these changes there are two major aspects of CNT enhancement to the composites. On the one hand, CNT 3D networks not only lead to a strongly-enhanced cohesion in matrix but refine the PyC crystalline grain to prevent annular cracks from thermal stress. The long pull-out of fibers is also attribute to the axial direction deflection of cracks, which improves the application efficiency of fibers in the tensile process. In this sense, CNT plays an assistance role to strengthen and toughen the composites on microscale. On the other hand, CNTs bear the load then pull out from matrix and break causing a rougher surface of fracture. This way, CNT offers a nanoscale reinforcement directly and as a complementary effect to the higher strength. The two kinds of reinforcement mechanisms act on the composites directly or indirectly to distribute stress and dissipate energy, which optimizes the composites structure and achieves significant improvement of composites strength and toughness.

3.4 Tensile behaviors of composites after heat treatment

After heat treatment the strength of composites (Fig. 8(a)) increases by 4.36% for pure C/Cs but 25.68% for CNTs-C/Cs. It is logical to believe that annealing makes a promotion to the reinforcement of CNT in composites. In pure C/Cs, graphitization causes more microstructure defects such as F/M interface debonding and cracks in matrix. These defects disrupt the integration in composites and hinder the stress transfer through F/M interface and provide plenty of channels for cracks growing. Compared with pure C/Cs, the presence of CNT almost makes the matrix of CNTs-C/Cs maintain the integrity and continuity during the heat

treatment and leads to a high anti-destroy capability. The annealing achieves a larger La due to the stress graphitization of CNT and endows matrix with the ability of anti-crack in plane. In this way, an anti-tensile matrix forms after heat treatment and help composites reach optimal performance. Besides, after graphitization, there exists a weak F/M interface in both composites due to the thermal stress. The propagation of cracks is easy to deflect into axial direction of fibers, and it is beneficial to the detaching of PyC from fibers during the tensile process. This may be the reason for a slight increase of tensile strength of pure C/Cs. In HT-CNTs-C/Cs, the interface between CNT and PyC also degrades properly and causes a longer pull-out of CNT during the tensile tests[33]. The two kinds of weakening in interface not only open up new channels of energy consumption but change the fracture of HT-CNTs-C/Cs. The fracture surface is shown in Fig. 8(b) with more concrete information. A single crack in matrix deflects when it propagates to the weak interface, and after a long distance propagation in the interface it comes across some defects of PyC then transfers to matrix continuously. A series of propagation-deflection circulations between interface and matrix make a lot of step-like fracture as pointed by arrows which is another mechanism to toughen and strengthen the composites.

Two conclusions can be drawn from these improvements. Firstly, CNT can enhance the tensile strength before and after heat treatment and secondly, the great enhancement of tensile strength after adding CNT and heat treatment is indeed attribute to the following two mechanisms: refinement of PyC matrix and change of fracture mode. As described in Fig. 9(a)-(d), the presence of CNT results in a smaller La but fewer in-plane defects and smaller

interlayer spacing (d_{002}) in PyC crystallite. The improvement of PyC microstructure attributed to the CNT increases the tensile strength in some degree. However, a small La is also unexpected and has some negative effects to the mechanical performance. Annealing solves the problem properly not only by enlarging La significantly but a further decrease of in-plane defects and interlayer spacing. These refinements makes it hard to destroy the PyC, so there are few cracks in matrix in HT-CNTs-C/Cs, and also, it indeed realizes a remarkable increase of tensile strength. Besides, Fig. 9(e)-(h) show that adding CNT changes the brittle fracture into pseudo-plastic fracture. In CNT reinforced C/Cs before and after heat treatment, an axial direction deflection of cracks makes a debonding of fibers and increases utilization of both fibers and F/M interface efficiently. The deflection of cracks propagation also disperses the energy and each component of composites suffers a diluted energy, so the ability of anti-destroy of the whole composites is increased. In HT-CNTs-C/Cs, a step-like fracture, longer pull-outs of CNTs (local area magnification in Fig. 9(h)) and more channels of energy consumption (direction of arrows in Fig. 9(h)) are the evidence of a high-efficiency employ of fibers, interfaces and CNT simultaneous, and these are reasons for the increase of tensile strength and toughness.

4. Conclusions

In this work, the tensile strength of CNTs-C/Cs increased by 14.2% and 30.5% for the CNT contents of 0.9 wt% and 1.5 wt%, respectively, with which decreased by 18.3% for 2.4 wt%. The work of fracture and Young's modulus as well as tensile strength achieved optimum performance when CNT content was 1.5 wt%. It was found that the presence of CNT not only

changed the microstructure of PyC to maintain an anti-destructive matrix of C/Cs but changed the fracture mode of tensile tests to strengthen and toughen the C/Cs.

After heat treatment, the tensile strength of CNTs-C/Cs increased by 25.68%, much higher than 4.36% of pure C/Cs, indicating that heat treatment promoted the strengthening and toughening effect of CNT. The L_a value of CNTs-C/Cs increased rapidly from 3.08 nm to 4.49 nm, further enhancing the in-plane tensile strength of PyC. The larger L_a and the step-like fracture morphology enabled HT-CNTs-C/Cs to have the highest strength among the four kinds of composites.

The existence of CNTs not only improved the microstructure of PyC and enhanced the ability of CNTs-C/Cs against destruction, but also opened a new way of energy consumption, thus the fibers and the interface being fully utilized. Heat treatment strengthened the influence of CNTs on the properties of the composites. The suggested mechanism of CNTs in strengthening and toughening the C/Cs provides a guidance for the preparation of C/Cs of high strength and high toughness.

Acknowledgements

This work is supported by the National Natural Science Foundation of China (Nos.51502242, 51432008, and U1435202); Shanghai Aerospace Science and Technology Innovation Foundation (No. SAST201470), and the Research Fund of State Key Laboratory of Solidification Processing (NWPU), China (Grant no. 142-TZ-2016).

References

[1] L. Feng, K.Z. Li, Z.Z. Zhao, H.J. Li, L.L. Zhang, J.H. Lu, Q. Song, Three-dimensional

carbon/carbon composites with vertically aligned carbon nanotubes: Providing direct and indirect reinforcements to the pyrocarbon matrix, *Mater. Des.* 92 (2016) 120-128.

[2] L. Feng, K.Z. Li, J.J. Sun, Y.J. Jia, H.J. Li, L.L. Zhang, Influence of carbon nanotube extending length on pyrocarbon microstructure and mechanical behavior of carbon/carbon composites, *Appl. Surf. Sci.* 355 (2015) 1020-1027.

[3] P. Xiao, X.F. Lu, Y.Q. Liu, L.H. He, Effect of in situ grown carbon nanotubes on the structure and mechanical properties of unidirectional carbon/carbon composites, *Mater. Sci. Eng. A* 528(7-8) (2011) 3056-3061.

[4] Q. Song, K.Z. Li, H.L. Li, H.J. Li, C. Ren, Grafting straight carbon nanotubes radially onto carbon fibers and their effect on the mechanical properties of carbon/carbon composites, *Carbon* 50(10) (2012) 3949-3952.

[5] E.T. Thostenson, Z.F. Ren, T.W. Chou, Advances in the science and technology of carbon nanotubes and their composites: a review, *Compos. Sci. Technol.* 61(13) (2001) 1899-1912.

[6] F.V. Ferreira, W. Franceschi, B.R.C. Menezes, F.S. Brito, K. Lozano, A.R. Coutinho, L.S. Cividanes, G.P. Thim, Dodecylamine functionalization of carbon nanotubes to improve dispersion, thermal and mechanical properties of polyethylene based nanocomposites, *Appl. Surf. Sci.* 410 (2017) 267-277.

[7] W. Shen, R. Ma, A. Du, X. Cao, H. Hu, Z. Wu, X. Zhao, Y. Fan, X. Cao, Effect of carbon nanotubes and octa-aminopropyl polyhedral oligomeric silsesquioxane on the surface behaviors of carbon fibers and mechanical performance of composites, *Appl. Surf. Sci.* 447 (2018).

- [8] Q. Guan, L. Yuan, Y. Zhang, A. Gu, G. Liang, Tailoring the structure of aligned carbon nanotube bundle by reactive polymer for strengthening its surface interaction with thermosets and the excellent properties of the hybrid thermosets, *Appl. Surf. Sci.* 439 (2018) 638-648.
- [9] J. Zhao, L. Liu, Q. Guo, J. Shi, G. Zhai, J. Song, Z. Liu, Growth of carbon nanotubes on the surface of carbon fibers, *Carbon* 46(2) (2008) 380-383.
- [10] H. Qian, A. Bismarck, E.S. Greenhalgh, G. Kalinka, M.S.P. Shaffer, Hierarchical composites reinforced with carbon nanotube grafted fibers: The potential assessed at the single fiber level, *Chem. Mater.* 20(5) (2008) 1862-1869.
- [11] Q.M. Gong, Z. Li, X.W. Zhou, J.J. Wu, Y. Wang, J. Liang, Synthesis and characterization of in situ grown carbon nanofiber/nanotube reinforced carbon/carbon composites, *Carbon* 43(11) (2005) 2426-2429.
- [12] Q. Song, K.Z. Li, L.H. Qi, H.J. Li, J.H. Lu, L.L. Zhang, Q.G. Fu, The reinforcement and toughening of pyrocarbon-based carbon/carbon composite by controlling carbon nanotube growth position in carbon felt, *Mater. Sci. Eng. A* 564 (2013) 71-75.
- [13] H. Qian, A. Bismarck, E.S. Greenhalgh, M.S.P. Shaffer, Synthesis and characterisation of carbon nanotubes grown on silica fibres by injection CVD, *Carbon* 48(1) (2010) 277-286.
- [14] Q. Song, K.Z. Li, L.L. Zhang, L.H. Qi, H.J. Li, Q.G. Fu, H.L. Deng, Increasing mechanical strength retention rate of carbon/carbon composites after graphitization by grafting straight carbon nanotubes radially onto carbon fibers, *Mater. Sci. Eng. A* 560 (2013) 831-836.
- [15] R.J. Sager, P.J. Klein, D.C. Lagoudas, Q. Zhang, J. Liu, L. Dai, J.W. Baur, Effect of carbon nanotubes on the interfacial shear strength of T650 carbon fiber in an epoxy matrix,

Compos. Sci. Technol. 69(7-8) (2009) 898-904.

[16] V.P. Veedu, A.Y. Cao, X.S. Li, K.G. Ma, C. Soldano, S. Kar, P.M. Ajayan, M.N. Ghasemi-Nejhad, Multifunctional composites using reinforced laminae with carbon-nanotube forests, *Nat. Mater.* 5(6) (2006) 457-462.

[17] A. Gao, C. Su, S. Luo, Y. Tong, L. Xu, Densification mechanism of polyacrylonitrile-based carbon fiber during heat treatment, *J. Phys. Chem. Solids* 72(10) (2011) 1159-1164.

[18] M. Guellali, R. Oberacker, M.J. Hoffmann, Influence of heat treatment on microstructure and mechanical properties of CVI-CFC composites with medium and highly textured pyrocarbon matrices, *Compos. Sci. Technol.* 68(5) (2008) 1115-1121.

[19] Q. Song, K.Z. Li, H.J. Li, S.Y. Zhang, L.H. Qi, Q.G. Fu, A novel method to fabricate isotropic pyrocarbon by densifying a multi-walled carbon nanotube preform by fixed-bed chemical vapor deposition, *Carbon* 59 (2013) 547-550.

[20] Q.M. Gong, L. Zhi, X.D. Bai, D. Li, J. Liang, The effect of carbon nanotubes on the microstructure and morphology of pyrolytic carbon matrices of C-C composites obtained by CVI, *Compos. Sci. Technol.* 65(7-8) (2005) 1112-1119.

[21] A.C. Ferrari, J. Robertson, Interpretation of Raman spectra of disordered and amorphous carbon, *Phys. Rev. B* 61(20) (2000) 14095-14107.

[22] O.M. Marago, F. Bonaccorso, R. Saija, G. Privitera, P.G. Gucciardi, M.A. Iati, G. Calogero, P.H. Jones, F. Borghese, P. Denti, V. Nicolosi, A.C. Ferrari, Brownian Motion of Graphene, *Acs Nano* 4(12) (2010) 7515-7523.

- [23] A. Yoshida, Y. Kaburagi, Y. Hishiyama, Full width at half maximum intensity of the G band in the first order Raman spectrum of carbon material as a parameter for graphitization, *Carbon* 44(11) (2006) 2333-2335.
- [24] K. Matsui, L.J. Lanticse, Y. Tanabe, E. Yasuda, M. Endo, Stress graphitization of C/C composite reinforced by carbon nanofiber, *Carbon* 43(7) (2005) 1577-1579.
- [25] L.J. Lanticse-Diaz, Y. Tanabe, T. Enami, K. Nakamura, M. Endo, E. Yasuda, The effect of nanotube alignment on stress graphitization of carbon/carbon nanotube composites, *Carbon* 47(4) (2009) 974-980.
- [26] Y. Zhao, Z.J. Liu, H.Q. Wang, J.L. Shi, J.C. Zhang, Z.C. Tao, Q.G. Guo, L. Liu, Microstructure and thermal/mechanical properties of short carbon fiber-reinforced natural graphite flake composites with mesophase pitch as the binder, *Carbon* 53 (2013) 313-320.
- [27] K. Bogdanov, A. Fedorov, V. Osipov, T. Enoki, K. Takai, T. Hayashi, V. Ermakov, S. Moshkalev, A. Baranov, Annealing-induced structural changes of carbon onions: High-resolution transmission electron microscopy and Raman studies, *Carbon* 73 (2014) 78-86.
- [28] A. Sadezky, H. Muckenhuber, H. Grothe, R. Niessner, U. Poschl, Raman micro spectroscopy of soot and related carbonaceous materials: Spectral analysis and structural information, *Carbon* 43(8) (2005) 1731-1742.
- [29] P. Koskinen, S. Malola, H. Haekkinen, Evidence for graphene edges beyond zigzag and armchair, *Phys. Rev. B* 80(7) (2009).
- [30] L.G. Cancado, M.A. Pimenta, B.R.A. Neves, M.S.S. Dantas, A. Jorio, Influence of the

atomic structure on the Raman spectra of graphite edges, *Phys. Rev. Lett.* 93(24) (2004).

[31] H. Mei, H.W. Wang, N. Zhang, H. Ding, Y.T. Wang, Q.L. Bai, Carbon nanotubes introduced in different phases of C/PyC/SiC composites: Effect on microstructure and properties of the materials, *Compos. Sci. Technol.* 115 (2015) 28-33.

[32] H. Mei, Q. Bai, T. Ji, H. Li, L. Cheng, Effect of carbon nanotubes electrophoretically-deposited on reinforcing carbon fibers on the strength and toughness of C/SiC composites, *Compos. Sci. Technol.* 103 (2014) 94-99.

[33] H. Mei, Q. Bai, Y. Sun, H. Li, H. Wang, L. Cheng, The effect of heat treatment on the strength and toughness of carbon fiber/silicon carbide composites with different pyrolytic carbon interphase thicknesses, *Carbon* 57 (2013) 288-297.

List of figure and table captions

Fig. 1 SEM morphologies of (a) 0.9 wt%, (b) 1.5 wt% and (c) 2.4 wt% CNT doped carbon fibers; (d) High magnification of CNT; (e) TEM images of CNT; (f) high-resolution TEM of CNT.

Fig. 2 PLM images of composites. (a) pure C/Cs; (b) CNTs-C/Cs-1.5; (c) HT-C/Cs; (d) HT-CNTs-C/Cs-1.5.

Fig. 3 Raman spectra of composites. (a) typical spectra of each series; (b) decompositions of Raman spectra of the first order for as-deposited CNTs-C/Cs-1.5.

Fig. 4 Tensile behaviors of composites before heat treatment. (a) The typical stress-strain curves of C/Cs with different CNTs contents; (b) Tensile strength of C/Cs with different CNTs contents.

Fig. 5 Changes in (a) Young's modulus and (b) work of fracture of C/Cs with different CNTs contents.

Fig. 6 SEM images of the fracture surface of C/Cs with different CNTs contents. (a) Pure C/Cs; (b) CNTs-C/Cs-0.9; (c) CNTs-C/Cs-1.5; (d) CNTs-C/Cs-2.4.

Fig. 7 High resolution SEM images of fracture surface of composites. (a) Pure C/Cs; (b) CNT pull out of CNTs-C/Cs; (c), (d) porous structure formed in CNTs-C/Cs-2.4.

Fig. 8 Tensile behaviors of composites after heat treatment (a) tensile strength of pure C/Cs and CNTs-C/Cs-1.5 after 2100°C heat treatment; (b) SEM image of CNTs-C/Cs-1.5 after 2100°C heat treatment.

Fig. 9 Schematic diagram of the strengthen and toughen mechanisms of CNT. (a), (b), (c), (d)

microstructure changes of C/Cs, CNTs-C/Cs, HT-C/Cs, HT-CNTs-C/Cs; (e), (f), (g), (h)

fracture mode changes of C/Cs, CNTs-C/Cs, HT-C/Cs, HT-CNTs-C/Cs.

Accepted manuscript

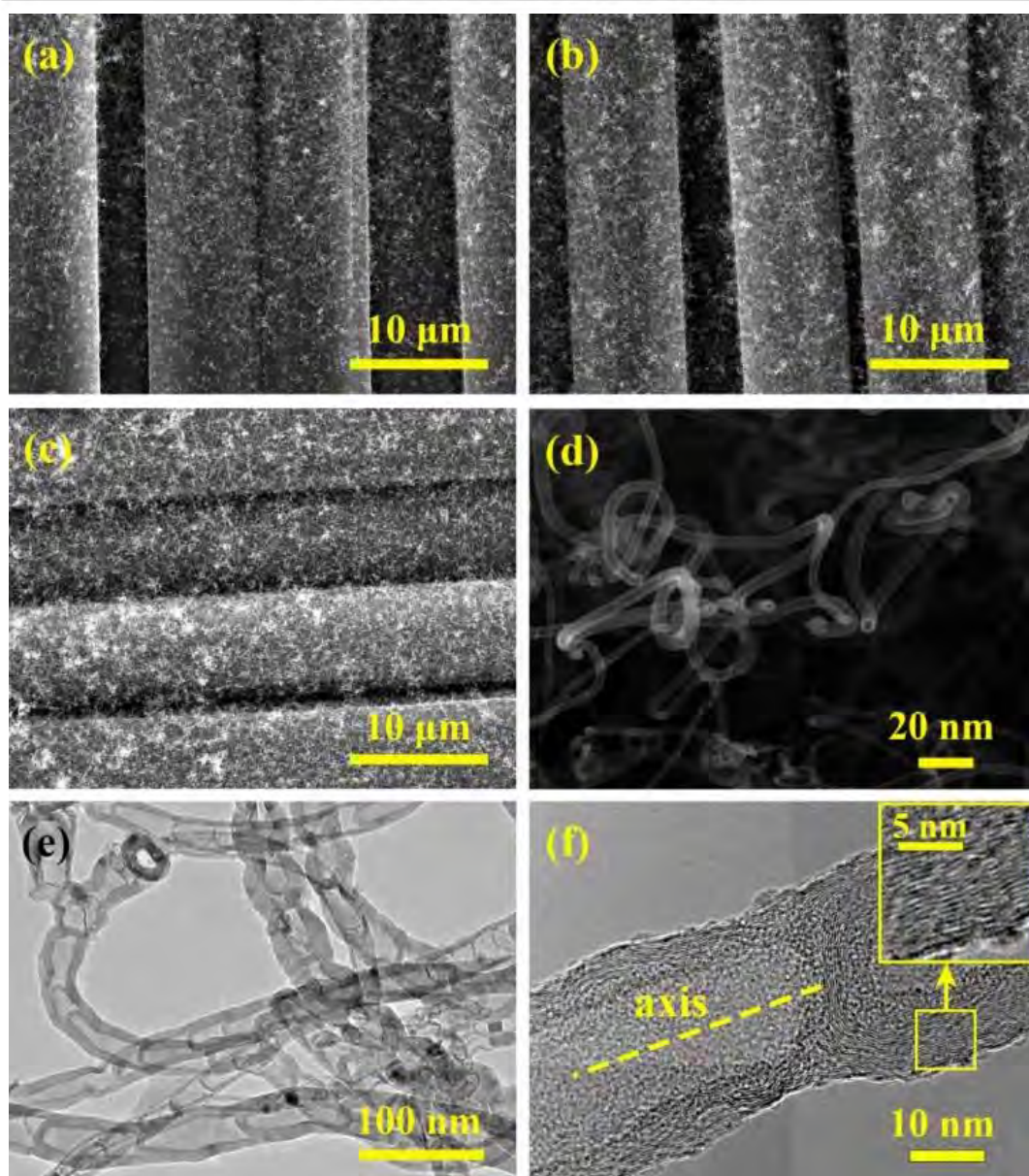


Fig.1

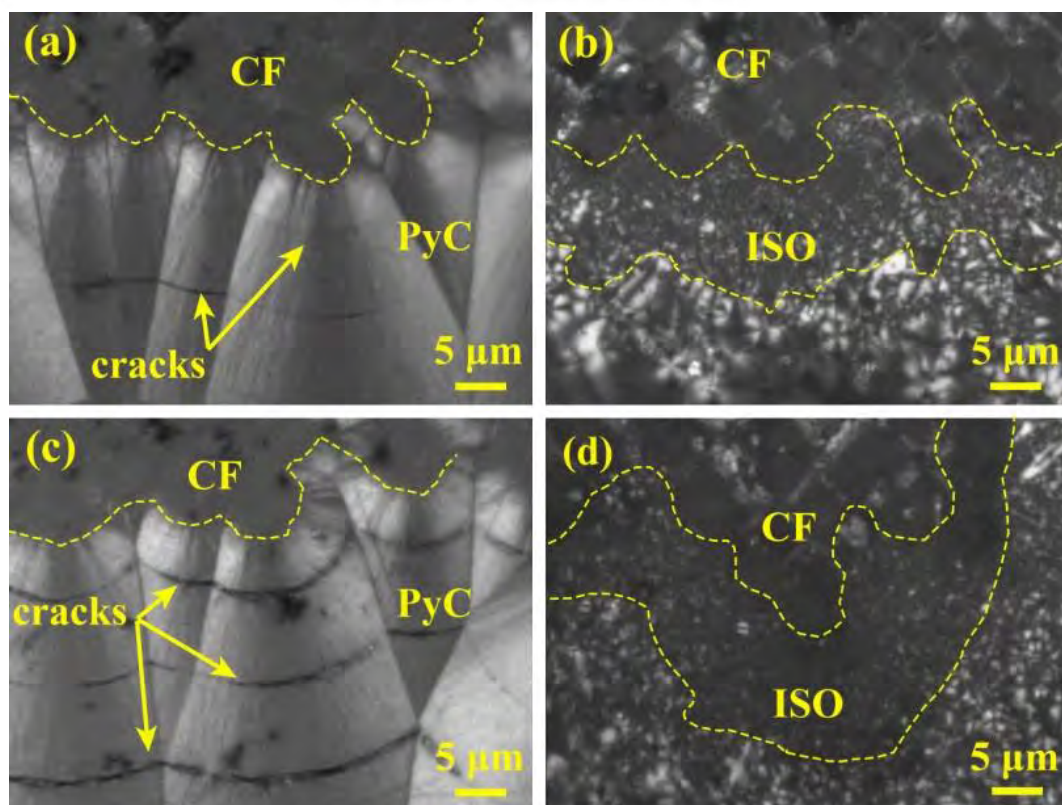
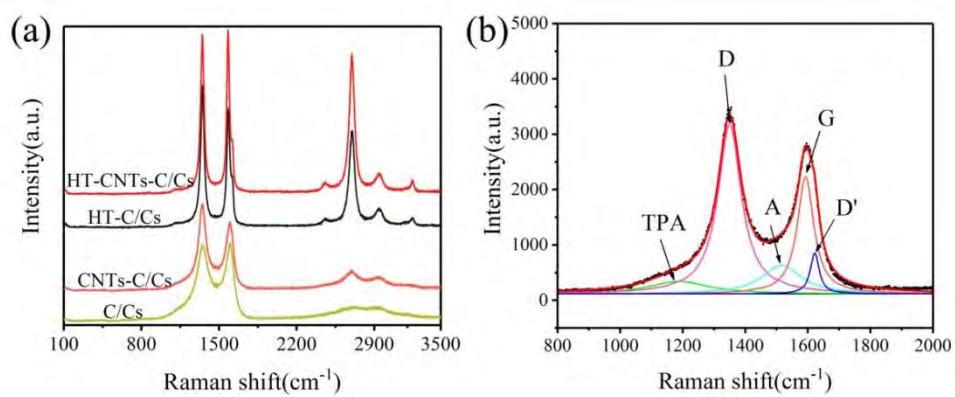
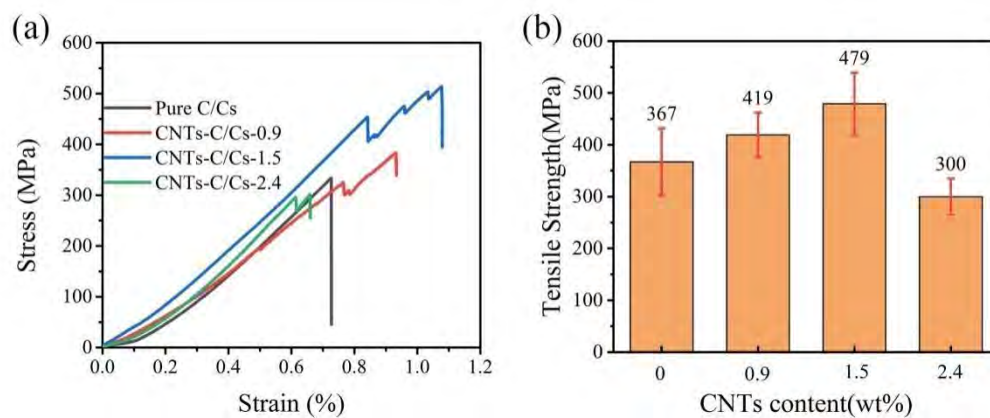


Fig.2

**Fig.3**

Accepted manuscript

**Fig.4**

Accepted manuscript

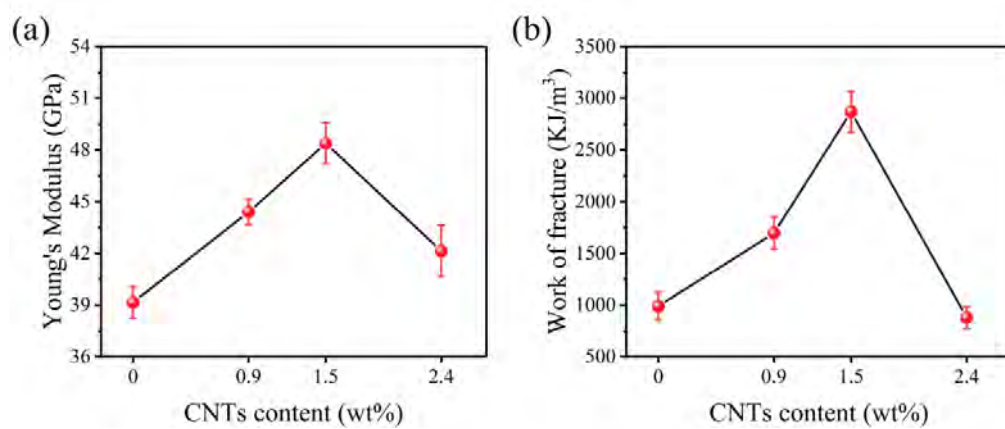


Fig.5

Accepted manuscript

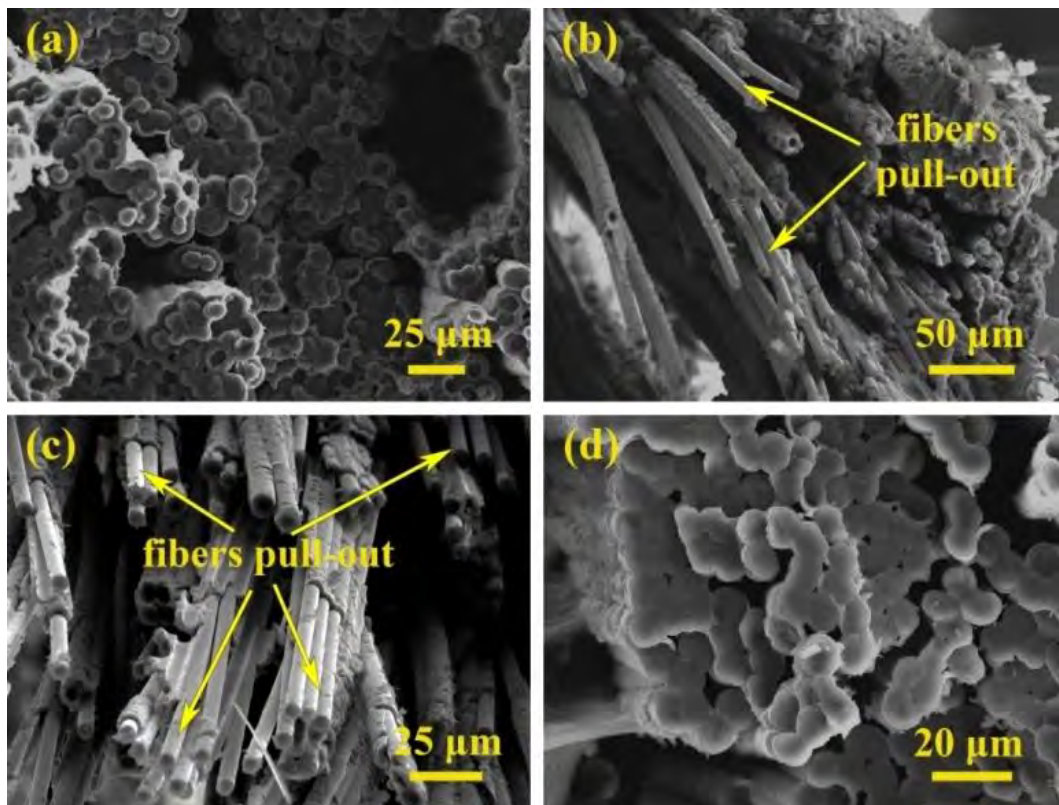


Fig.6

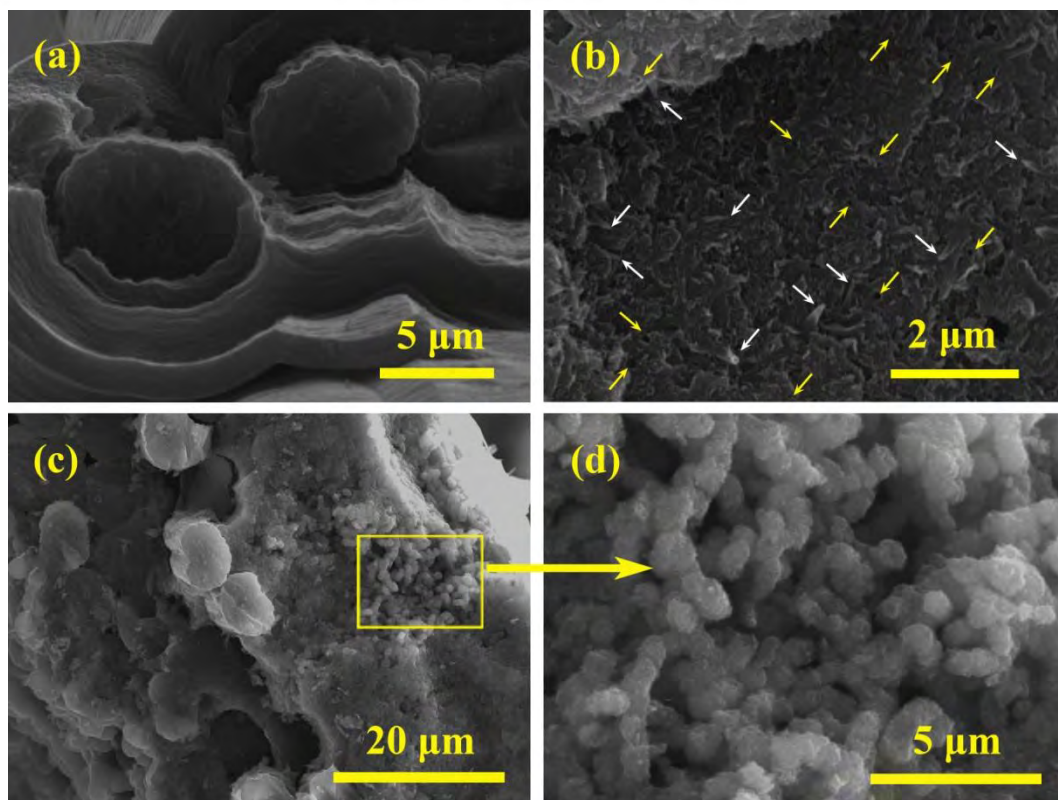


Fig.7

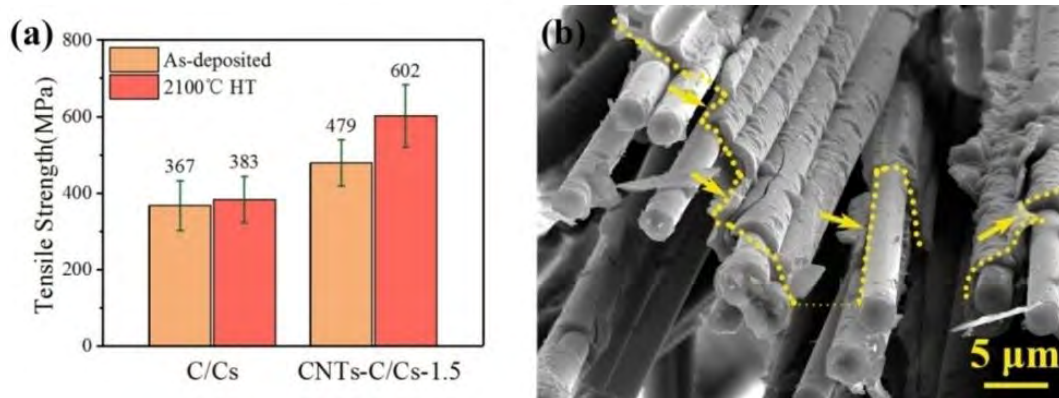


Fig.8

Accepted manuscript

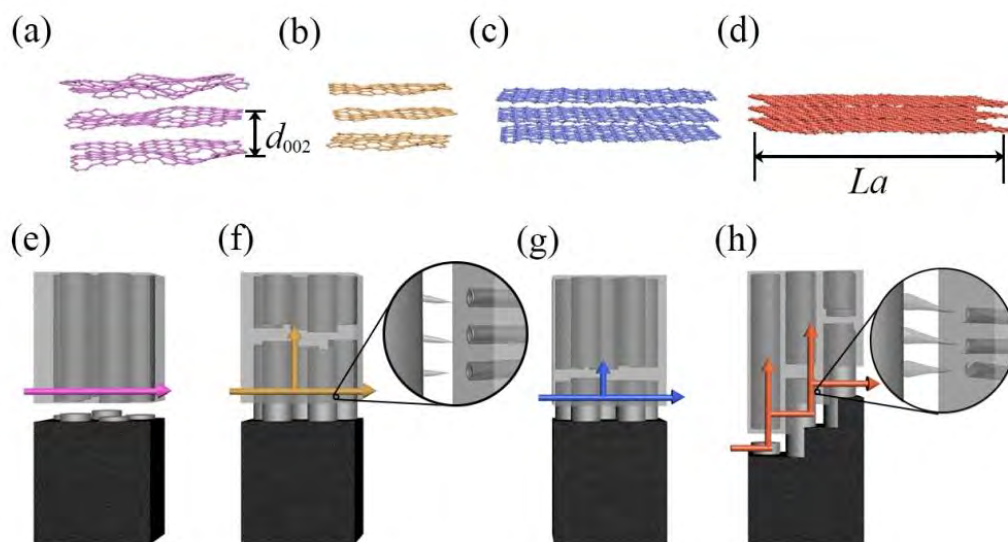


Fig.9

Table 1 Structure parameters obtained from the first order of Raman spectra of four kinds of composites.

Table 2 Statistical results of tensile strength, Young's modulus and work of fracture of composites with different contents of CNTs.

Accepted manuscript

Table 1

Materials	I_{TPA}/I_G	I_A/I_G	I_D/I_G	I_D^*/I_G^*	$La(\text{nm})$	FWHM-G(cm^{-1})
C/Cs	0.56±0.013	0.77±0.021	0.29±0.015	1.27±0.04	3.46±0.09	70.13±11.51
CNTs-C/Cs	0.37±0.011	0.54±0.036	0.19±0.002	1.43±0.06	3.08±0.12	65.13±5.50
HT-C/Cs	0.08±0.002	0.07±0.003	0.17±0.005	1.21±0.02	3.64±0.07	34.53±6.71
HT-CNTs-C/Cs	0.06±0.004	0.05±0.002	0.16±0.005	0.98±0.01	4.49±0.06	28.09±3.29

Accepted manuscript

Table 2

Content of CNTs (wt %)	Tensile stress (MPa)	Young's modulus (GPa)	Work of fracture (KJ/m ³)	Apparent density (g/cm ³)
0	367±65	39.15±0.91	988.83±135.22	1.65±0.04
0.9	419±43	44.40±0.73	1696.23±156.67	1.66±0.02
1.5	479±60	48.38±1.25	2870.22±195.01	1.68±0.04
2.4	300±35	42.13±1.49	879.23±103.46	1.63±0.03

Accepted manuscript